Original Article

Biofpr Biofuels Bioproducts & Biorefining

Production and characterization of cellulose acetate using olive tree pruning biomass as feedstock

José Antonio Rodríguez-Liébana, Andaltec I+D+i, Plastic Technological Centre, Martos, Spain
Esther Robles-Solano, Department of Chemical, Environmental and Materials Engineering, University of Jaén, Jaén, Spain
Sofia Jurado-Contreras, Andaltec I+D+i, Plastic Technological Centre, Martos, Spain
Francisca Morillas-Gutiérrez, Department of Chemical, Environmental and Materials Engineering, University of Jaén, Jaén, Spain
Alberto J. Moya, Soledad Mateo, Department of Chemical, Environmental and Materials Engineering, University of Jaén, Jaén, Spain; University Institute for Research in Olive Grove and Olive Oil (INUO), University of Jaén, Jaén, Spain
Francisco Javier Navas-Martos, Andaltec I+D+i, Plastic Technological Centre, Martos, Spain
M. Dolores La Rubia, Department of Chemical, Environmental and Materials Engineering, University of Jaén, Jaén, Spain; University Institute for Research in Olive Grove and Olive Oil (INUO), University of Jaén, Jaén, Spain

Received November 22 2023; Revised January 7 2024; Accepted January 22 2024;
View online at Wiley Online Library (wileyonlinelibrary.com);
DOI: 10.1002/bbb.2600; *Biofuels, Bioprod. Bioref.* (2024)

Abstract: Olive tree pruning (OTP) is one of the most abundant sources of biomass waste in the Mediterranean basin. This is especially relevant in southern Spain where olive oil production represents a large part of the economy. Olive tree prunings are mostly either burned or are spread in olive orchards as an organic amendment, or used for heat generation on a domestic scale. However, the lignocellulosic composition of OTP makes it a potential source of biopolymers, thus providing an excellent economic alternative for the olive oil sector. In this work, pretreated OTP fibers were subjected to an optimized alkaline treatment followed by a single-step bleaching reaction with H_2O_2. Afterwards, the cellulose pulp was transformed chemically to obtain cellulose acetate. Noncellulosic components were removed effectively from OTP, thus obtaining a pulp highly purified in cellulose with 71% crystallinity and 355 °C maximum degradation temperature. Nevertheless, a very large amount of cellulose (ca. 50%) was eliminated throughout the process, especially during acid pretreatment, which was responsible for 38% solubilization. A similar level of acetylation and degree of substitution was obtained by using acetylation times in the range of 1 to 6 h. No large differences were observed in the infrared spectra and X-ray diffractograms of the synthesized acetates. However, their thermal stability varied significantly with reaction time, evolving from a multistep degradation pattern to a single and sharp peak between 300 and 400 °C with increasing time. Thermogravimetric curves revealed that at least 5 h (preferably 6 h) were

Correspondence to: M. Dolores La Rubia, Department of Chemical, Environmental and Materials Engineering, University of Jaén, Campus Las Lagunillas, Jaén 23071, Spain. E-mail: mdrubia@ujaen.es

needed to obtain cellulose acetate from OTP with adequate thermal stability for further processing.

Key words: lignocellulose; waste biomass; waste valorization; biopolymers

Introduction

In recent years, the use of agricultural residues for high added-value applications has been strengthened as they are generated in large quantities and their accumulation often poses a problem. These residues have negative impacts in agriculture as they are generated at a rapid rate and generally affect many agricultural activities, people, and spaces. Accumulated residues can temporarily immobilize nutrients, affecting soil health and requiring additional fertilizers.[1,2] Excessive residue accumulation disrupts farming operations, reducing the efficiency of machinery and increasing labor. Dry residues in hot climates create fire hazards, risking crop loss and property damage. Runoff water carrying residues contributes to water pollution, affecting aquatic ecosystems. Residues in farming communities impact aesthetics and social well-being. Land-use conflicts arise as residue management competes with other purposes in limited spaces. Improper residue management releases greenhouse gases, contributing to climate change.[3]

The utilization of lignocellulosic residues as raw materials for bio-based applications has been on the rise, presenting itself as a promising and essential alternative for the functioning of modern industrial societies.[2] Their appeal as a sustainable source of biomaterials is largely attributed to different factors such as their low cost, widespread availability, and chemical composition. Agro-industrial residues primarily consist of cellulose (30–60%), hemicellulose (14–40%), and lignin (7–20%).[4] Nevertheless, it is difficult to achieve 100% revalorization of lignocellulose because the revalorization strategy is dependent on the targeted products. Cellulose serves as a fundamental structural component in plants, representing the most abundant renewable resource in nature. A diverse range of processes have been explored to extract and purify cellulose from agro-industrial residues, depending on the chemical nature of the raw material. The incorporation of pretreatment techniques aims primarily at breaking and fractionating the components of lignocellulosic biomass, thereby opening the material's structure and enhancing the accessibility of the cellulose microfibrillar structure for its subsequent isolation. A typical approach involves conditioning steps, pretreatments for fiber swelling, acid or alkaline hydrolysis, and subsequent purification steps by bleaching reactions. Once extracted, cellulose may be transformed into a wide variety of derivatives including ethers, esters or nanocellulose with application in different sectors, such as food packaging[5] or water purification.[6] Hemicellulose is less resistant than cellulose to chemical attack. After partial or total depolymerization, it can be potentially deemed to be a source of multiple products such as bioethanol and biofuel, xylo-oligosaccharides, xylitol, sorbitol, packaging films, adsorbents, functional ingredients for foods and pharmaceuticals, production of bioplastics and biocomposites, and so forth.[7,8] Lignin can be used as a source of value-added chemicals such as hydroxycinnamic acids or phenolic antioxidants, and as a starting material for a series of products including dispersant, emulsificant and chelant agents, activated charcoal, adhesives and fertilizers.[9] Lignin is also being currently conceived as a building block for the manufacturing of bio-based polymers,[10,11] or in bio-based biocide delivery system.[12] Robinson *et al.* (2022)[13] performed a process multistructure to evaluate the techno-economical viability of lignin valorization for a plant scale of 150 kt/year, focusing on the production of aromatic monomers, phenols-formaldehyde resins and aromatic aldehyde/acids.[13]

Among the chemical treatments for lignocellulose fractionation, alkaline hydrolysis is commonly employed for cellulose extraction both as pretreatment or as the main treatment step, due to its applicability under mild conditions and low risk. However, it possesses some drawbacks including extended processing times. These challenges can be mitigated by combining the alkaline treatment with other methods.[14] The bleaching process is usually an integral part of cellulose purification and aims to achieve precise removal of lignin in unpurified cellulose pulp, resulting in a more uniform final product. In most instances, bleaching is accomplished by treating the fiber with chlorine in an acidic medium.[15]

Due to its structural arrangement, cellulose possesses certain properties that restrict its direct application, such as high hydrophilicity, low solubility in common solvents, low dimensional stability, and a high melting temperature. To address these limitations, cellulose is typically transformed into derivatives like cellulose acetate, nitrocellulose, methylcellulose, and carboxymethyl cellulose. Among them, cellulose acetate is distinguished by its compostable and biodegradable characteristics, making it an excellent choice for producing food packaging materials, textile fibers, paints,

photographic films, medical and pharmaceutical products,[16] filtration membranes,[17] bioremediation,[18,19] and membranes for drug delivery systems.[20] The versatility of cellulose acetate in these applications helps to reduce the dependence on fossil fuels in various industrial sectors.[21]

Various lignocellulosic materials from agricultural activity have been identified as potential sources for the production of cellulose acetate, encompassing flamboyant fruit pods,[22] rice husk,[23] cotton by-products,[24] coconut shell,[25] sugarcane bagasse,[26,27] and oil palm empty fruit bunch.[28] In Spain, the intensive production of olive oil generates an annual volume of approximately 3 t ha^{-1} of olive tree pruning (OTP) biomass waste. Traditionally, this residue is used *in situ* as a soil amendment, or in most cases it is incinerated, significantly increasing the carbon footprint of the olive oil industry. This has promoted the use of this agricultural waste in the industrial sector.

The province of Jaén (in south Spain) is characterized by having over 6 000 000 ha of olive plantations (25% of the total in Spain), representing more than 40% of the olive oil production in the Spanish territory. Consequently, a large amount of OTP waste is generated annually. The revalorization of OTP, not only in the south of Spain but also in all the Mediterranean Basin, is particularly relevant. Given its lignocellulosic composition in which cellulose represents approximately 30–40%,[29] OTP is a potential candidate for the extraction and subsequent chemical transformation of its cellulosic fraction, and further utilization across diverse industrial sectors. In this study, the extraction and purification of cellulose from OTP by a three-step process was firstly addressed. The experimental conditions of the alkaline hydrolysis were optimized through response surface methodology (RSM) to ensure maximum delignification of OTP fibers. The purified cellulose pulp obtained was subsequently used for the synthesis of cellulose acetate by conventional heterogeneous reaction with acetic anhydride, paying especial attention to the effect of acetylation time. The properties of both the solids produced during cellulose isolation and cellulose acetate samples synthesized at different reaction times were characterized by infrared spectroscopy, X-ray diffraction and thermogravimetric analysis.

Materials and methods

Extraction and purification of cellulose from OTP biomass

Selected branches of OTP biomass were collected from an orchard near the town of Martos (Jaén, south Spain) and subjected to a series of mechanical operations, both in cropland and in the laboratory, to obtain deleafed OTP fibers with particle size in the range 0.425–0.600 mm. The fibers were pretreated as obtained by stirring in an aqueous solution of 8% w/v nitric acid (HNO_3, 65–67% Puriss. p.a. ISO, (Reag. Ph. Eur.), Honeywell Chemicals, Madrid, Spain) at a temperature of 90 °C for 240 min. Under these conditions, the removal of hemicellulose and lignin was maximized, as well as the crystallinity of the remaining pulp.[29]

Table 1. Matrix of the experimental design performed considering NaOH concentration (*c*), reaction time (*t*) and reaction temperature (*T*) for the alkaline hydrolysis (coded and uncoded values).

Run	Coded			Uncoded		
	t	*T*	*c*	*t* (min)	*T* (°C)	*c* (%)
1	−1	−1	−1	90	65	4
2	1	−1	−1	120	65	4
3	−1	1	−1	90	85	4
4	1	1	−1	120	85	4
5	−1	−1	1	90	65	8
6	1	−1	1	120	65	8
7	−1	1	1	90	85	8
8	1	1	1	120	85	8
9	−1.41	0	0	83.85	75	6
10	1.41	0	0	126.15	75	6
11	0	−1.41	0	105	50.9	6
12	0	1.41	0	105	89.1	6
13	0	0	−1.41	105	75	3.82
14	0	0	1.41	105	75	6.82
15	0	0	0	105	75	6
16	0	0	0	105	75	6

The dried fibers were labeled as OTP-AH and stored in sealed bags until further treatment with aqueous solutions of sodium hydroxide (NaOH ≥98% (Reag. USP) p.a., ACS, ISO, ITW Reagents, Monza, Italy). Alkaline hydrolysis was performed at a solid/liquid ratio of 1:10 under different experimental conditions (Table 1). NaOH concentration (*c*), reaction time (*t*) and reaction temperature (*T*) were varied in order to achieve maximum delignification and minimum removal of cellulose. After finishing the reaction, the corresponding OTP-BH pulps were filtered, washed with abundant water until their pH was neutral, and dried at 105 °C for 16 h. Response surface methodology (RSM) was used to determine the best experimental conditions. The design of experiments approach consisted of a face-centered central composite design (FCCD) with 16 runs including two replicates in the central point in which *c*, *t* and *T* were the independent variables, and the concentrations of cellulose,

hemicellulose and lignin remaining in the solids were the response variables (Table 1). A numerical and graphical analysis of the data was carried out with Statistica v8.0 (Statsoft; Tulsa, OK, USA) and Design-Expert v6.0 (Stat-Ease Inc.; Minneapolis, MN, USA) software. The relationship between the response functions and the coded variables is described by the following second-degree polynomial equation:

$$Y = \beta_0 + \beta_i \sum x_i + \beta_{ii} \sum x_i^2 + \beta_{ij} \sum x_i x_j \quad (1)$$

where Y is the specific response function, x_i and x_j are independent variables, β_0 is a constant, and β_i, β_{ii} and β_{ij} are linear, quadratic and interactive coefficients, respectively.

The pulp obtained under optimized conditions of alkaline hydrolysis was further subjected to a bleaching reaction with 2% v/v H_2O_2 at a solid-to-liquid ratio of 1:20, at 70 °C for 60 min. The pH of the solution was adjusted between 11 and 12 by addition of NaOH 0.1 mol L^{-1}. Purified fibers (OTP-BL; hereafter also called cellulose) were filtered, washed with distilled water to remove the excess of reagents, dried, and milled to a particle size below 0.5 mm (Ultra Centrifugal Mill ZM 200; Retsch GmbH, Haan, Germany) before acetylation.

All the treatments were carried out in a 1 L glass reactor with mechanical stirring and temperature control. The yield of acid pretreatment (Y_{AH}), alkaline hydrolysis (Y_{BH}), and bleaching reaction (Y_{BL}) was calculated with the equations:

$$Y_{AH}(\%) = \frac{m_{OTP-AH}}{m_{OTP}} \times 100 \quad (2)$$

$$Y_{BH}(\%) = \frac{m_{OTP-BH}}{m_{OTP}} \times 100 \quad (3)$$

$$Y_{BL}(\%) = \frac{m_{OTP-BL}}{m_{OTP}} \times 100 \quad (4)$$

where m_{OTP}, $m_{OTP\text{-}AH}$, $m_{OTP\text{-}BH}$ and $m_{OTP\text{-}BL}$ are the weights (g) of raw OTP fibers, and after acid pretreatment, alkaline hydrolysis, and bleaching respectively.

The global yield was calculated with the Eqn (5):

$$Y_G(\%) = Y_{AH} \times Y_{BH} \times Y_{BL} \quad (5)$$

Acetylation of the extracted cellulose

The synthesis of cellulose acetate was carried out by the conventional heterogeneous process in which cellulose is reacted with acetic anhydride ($(CH_3CO)_2O \geq 99\%$ AGR ACS; Labkem, Murcia, Spain) in a medium composed of acetic acid ($CH_3COOH \geq 99\%$ AGR ACS; Labkem) and sulfuric acid (H_2SO_4 95–97% AGR ISO; Labkem) as the catalyzer. First, 2 g of the cellulose extracted previously (OTP-BL) was mixed with 70 mL CH_3COOH to swell the cellulose fibers. After 15 min, the fibers were activated for 30 min by adding 0.2 mL concentrated H_2SO_4 in 10 mL CH_3COOH. Subsequently, a volume of 30 mL of $(CH_3CO)_2O$ was added slowly and the mixture was left to react for a specific time, which varied between 1 and 6 h, to assess the effect of reaction time on the extent of acetylation and on the properties of the cellulose acetate that was formed. The reaction proceeded at constant temperature (40 °C) under magnetic stirring. The viscous solution of cellulose acetate was filtered, and 500 mL of cold distilled water (5 °C) was added to the filtrate to stop the reaction. This mixture was left to agitate for 1 h, and the precipitate formed was vacuum-filtered and washed with abundant water and ethanol to remove excess of CH_3COOH and $(CH_3CO)_2O$. Finally, the solid, labeled as OTP-CAx (x = 1–6), was dried at 60 °C overnight.

Characterization of OTP-cellulose and cellulose acetate samples

Compositional analysis

The moisture content of OTP biomass was calculated by subjecting the sample (5 replicates of approximately 2 g each) to oven drying at 105 °C until constant weight:

$$moisture\,(\%) = \frac{mo - m_{105}}{mo} \times 100 \quad (6)$$

where mo and m_{105} (g) are the weights of the sample before and after drying.

The chemical composition of the lignocellulosic materials was determined using the procedure developed by the National Renewable Energies Laboratory (NREL) for biomass analysis.[30] Around 2 g of the sample was transferred into a 50 mL glass flask containing 10 mL of a 72% w/w H_2SO_4 solution (ITW Reagents). The suspension was maintained at 60 °C in a water bath under gentle stirring for 7 min. Afterwards, the mixture was poured into a 1 L Erlenmeyer flask and diluted with 275 mL of distilled water. The flask was sealed and autoclaved for 45 min, and the resulting mixture was cooled at room temperature and filtered.

The solid residue remaining after acid hydrolysis was washed with distilled water and incinerated at 600 °C for 4 h to calculate acid insoluble lignin (AIL) following this equation:

$$AIL\,(\%) = \frac{m - m_{600}}{m} \times 100 \quad (7)$$

in which m (g) is the weight of the unhydrolyzed solid before incineration and, m_{600} (g) is the weight of the unhydrolyzed solid after incineration.

On the other hand, the polysaccharide content was determined after quantification of sugars in the hydrolyzate by high-performance liquid chromatography (HPLC). After filtration (0.22 µm syringe filters), a 20 µL aliquot of the hydrolyzate was injected into a Shimadzu Prominence Serie 20 chromatograph provided with an automatic injector (SIL-20ACHT) and a refraction index detector (RID-10A). Analyte separation was achieved in a Aminex HPX-87H chromatographic column (7.8 × 300 mm; Bio-Rad Laboratories Ltd., Hercules, CA, USA) with column temperature of 45 °C and an aqueous solution of H_2SO_4 5 mM as mobile phase (0.6 mL min^{-1} flow rate).

Fourier transform infrared spectroscopy

To identify the functional groups of the fibers and to monitor the process of cellulose extraction, raw OTP and the different OTP pulps were analyzed in a Fourier transform infrared (FTIR) spectrometer equipped with a deuterated triglycine sulfate detector (DTGS) (Tensor 27; Bruker, MA, USA), which is a detection system that works by transmittance. Fourier transform infrared spectroscopy was also used to assess the acetylation extent ($R_{FT\text{-}IR}$) and to calculate the degree of substitution ($DS_{FT\text{-}IR}$) of OTP-CA samples as in previous reports.[31–34] $DS_{FT\text{-}IR}$ is a parameter that indicates the quantity of hydroxyl groups in the cellulose chains that have been replaced by acetyl groups during the acetylation process. The acetylation extent refers to the degree or level to which acetylation has occurred, it specifically denotes the extent to which acetyl groups have replaced hydroxyl groups in the cellulose molecule. This method is based on the ratio between the area or the intensity of a peak attributed exclusively to acetylation (mostly the stretching of the C═O bond of acetyl group at 1730–1750 cm^{-1}), and that corresponding to the vibration of the C—O—C bond in the cellulose backbone (1020–1050 cm^{-1}) that remains unmodified after acetylation. $R_{FT\text{-}IR}$ and $DS_{FT\text{-}IR}$ were calculated with the following equations[31,32]:

$$R_{FT-IR} = \frac{I_{C=O}}{I_{C-O}} \tag{8}$$

$$WG_{FT-IR} = R_{FT-IR} \times 7.74 \tag{9}$$

$$DS_{FT-IR} = \frac{\left(WG_{FT-IR} + 10\right) \times 3}{17.74} \tag{10}$$

in which I_{C-O} and I_{C-O} represent the intensity of the peaks at 1730–1750 cm^{-1} and at 1020–1050 cm^{-1} respectively. The spectra were recorded in the region 4000–400 cm^{-1} with a wavenumber resolution of 4 cm^{-1} by using the attenuated total reflectance (ATR) method. For better comparison among samples, OPUS v6.5 software (Bruker, MA, USA) was used to maximize and stack the spectra.

X-ray diffraction

The crystalline structure of the different OTP fibers at each stage of treatment, as well as the changes produced after acetylation, was studied by X-ray diffraction (XRD). Before the analyses, the fibers were milled and passed through a 0.5 mm sieve (Ultra Centrifugal Mill ZM 200; Retsch GbmH, Haan, Germany). Powdered samples were placed on the holder and leveled to achieve total and even exposure to radiation. Measurements were performed in an X-Ray diffractometer (Empyrean; Malvern PANalytical) at room temperature with a monochromatic Cu-Kα radiation source at a rate of 2° min^{-1} in the 2θ range of 5–40°. The classical Segal method[35] was applied to calculate the crystallinity index (CrI):

$$CrI(\%) = \frac{I_{200} - I_{am}}{I_{200}} \times 100 \tag{11}$$

In this equation I_{200} is the maximum intensity of the (*200*) lattice diffraction peak corresponding to both amorphous and crystalline phases, and I_{am} represents the intensity scattered by the amorphous part. Both I_{200} and I_{am} are located at 2θ values of approximately 22° and 18° respectively.[36–40]

Thermogravimetric analysis

The thermal stability of the different fibers obtained during the experimental part (raw OTP, OTP-AH, optimized OTP-BH, OTP-BL and OTP-CA) was determined by thermogravimetric analysis (TGA) in TGA Q500 equipment (TA Instruments, New Castle, DE, USA) by weighing 10–20 mg of powdered sample in alumina pans. The derivative thermogravimetry (DTG) curves were also represented to assess the maximum degradation temperatures. All the measurements were carried out under a N_2 flow of 50 mL min^{-1} by heating the sample from room temperature to 1000 °C at a rate of 10 °C min^{-1}.

Results and discussion

Extraction and characterization of cellulose from OTP

Compositional analysis of OTP fibers. Optimization of alkaline hydrolysis

As reported in a previous work by the authors, raw OTP may be considered as a suitable lignocellulosic material

for cellulose isolation as it contains 31.53 wt.% of cellulose, 21.61 wt.% of hemicellulose and 24.76 wt.% of lignin.[29] After the acid pretreatment, a yellowish pulp with 63.32 wt.% of cellulose, 8.92 wt.% of hemicellulose and 7.78 wt.% of lignin was obtained (Fig. 1). This indicated an extensive removal of noncellulosic components (around 90%), which was the main objective of acid pretreatment. However, and taking into account the low mass of solid yielded at the end of the process (30.90 g per 100 g raw OTP), approximately 38% of the cellulose initially present in the OTP fibers was also hydrolyzed under the selected experimental conditions.[18]

After the acid pretreatment, OTP-AH fibers were subjected to alkaline hydrolysis, the conditions of which were optimized to maximize the removal of non-cellulosic components. Hemicellulose was not detected in most cases after the alkaline experiments (Table 2), thus impeding the application of the quadratic model. The only regression equations retrieved by the model here were therefore those for the concentrations of cellulose and lignin. Depending on the experimental conditions (Table 1), different grades of delignification were obtained after the treatments with NaOH. The resulting color changes arise from alterations in the chemical composition and the structure of the residue compounds. Removing lignins from agricultural residue, through chemical treatments, causes a shift in color by modifying or eliminating chromophores.[41] The color of OTP residues is also affected by various substances such as pigments, polyphenols, carotenoids, and chlorophyll.[42–44]

As shown in Table 2, the concentration of cellulose remaining in OTP-BH solids varied from 63.71% (run 3, in which the concentration of acid is the lowest) to 97.78% (run 14, in which the concentration of acid is the highest), whereas that of lignin oscillated from 5.26% (run 7) to 14.68% (run 4) respectively. Yields between 57.81% and 82.26% were obtained (Table 2).

The predicted quadratic regression equation for the concentrations of cellulose and lignin remaining in the solid (Eqns 12 and 13) are presented below. Figure 2 depicts the graphical representation of the experimental data against those predicted by the Eqns 12 and 13.

$$cellulose\ (wt.\%) = 93.25 + 3.95t - 2.52T + 3.60c - 6.53t^2 - 10.30T^2 + 4.25Tc \quad (12)$$

$$lignin\ (wt.\%) = 7.91 + 0.44t + 0.52T - 0.72c + 0.91t^2 - 1.35tT - 0.40tc - 2.09Tc \quad (13)$$

As shown in Fig. 2, the coefficients of determination were above 0.96 thus indicating that the quadratic regression model equations had good statistical validation for the prediction of the concentrations of cellulose and lignin remaining in OTP-BH fibers.[45] The effect of either *t*, *T*, or *c* on the response variables is reflected in the linear, quadratic, and interactive coefficients of the equations. The equations show that the three independent variables (linear terms) were significant for both response variables. Moreover, the values of the coefficients for lignin concentration were lower than those for the concentration of cellulose, likely due to the fact that the concentration of lignin in the fibers was already extensively reduced after acid pretreatment (OTP-AH had around 8% lignin).[29] As expected, an increase in *c* induced an increase in the concentration of cellulose. The terms *t* and especially *Tc* also had a positive influence in cellulose enrichment. However, the negative coefficient for *T* suggested that exposure of OTP-AH fibers to high temperatures during alkaline hydrolysis could lead to cellulose damage. This is supported by the negative value of the quadratic term T^2, which had the greatest effect on cellulose concentration. This is in line with the study by Melikoğlu *et al.*[45] who performed a similar optimization for the alkaline hydrolysis of apple pomace, and suggested that increased concentrations of NaOH, reaction time, and reaction temperature could damage the cellulose structure

Figure 1. Visual appearance of OTP fibers. From left to right: raw OTP, OTP-AH, OTP-BH, and OTP-BL.

Table 2. Chemical composition of the solids obtained after alkaline hydrolysis and yield of reaction.

Run	Moisture (%)	Cellulose (%)	Hemicellulose (%)	Lignin (%)	Yield (%)
1	5.853	74.38 ± 6.35	1.98 ± 0.44	7.70 ± 7.00	80.27
2	7.238	83.98 ± 6.70	2.49 ± 0.30	6.25 ± 0.56	82.26
3	6.297	63.71 ± 4.83	2.22 ± 0.74	9.74 ± 1.21	69.36
4	6.753	69.35 ± 10.90	1.74 ± 0.96	14.68 ± 3.43	66.41
5	7.972	75.85 ± 3.66	–	10.58 ± 1.89	80.29
6	8.729	81.43 ± 11.79	–	8.52 ± 0.32	76.68
7	8.260	79.08 ± 2.85	–	5.26 ± 0.68	62.56
8	7.299	86.89 ± 7.54	–	7.62 ± 2.67	58.90
9	8.588	72.82 ± 21.77	–	9.25 ± 0.43	71.38
10	7.680	86.09 ± 12.76	–	10.30 ± 1.55	61.91
11	6.996	76.80 ± 8.41	–	8.68 ± 0.92	57.81
12	7.648	67.11 ± 2.58	–	11.19 ± 0.013	60.10
13	7.174	89.78 ± 8.92	0.47 ± 0.05	8.77 ± 0.12	74.72
14	7.054	97.78 ± 3.22	–	7.14 ± 3.01	70.05
15	6.410	91.91 ± 2.75	0.09 ± 0.02	8.17 ± 2.85	72.08
16	6.103	93.81 ± 0.06	0.14 ± 0.20	7.55 ± 2.30	68.97

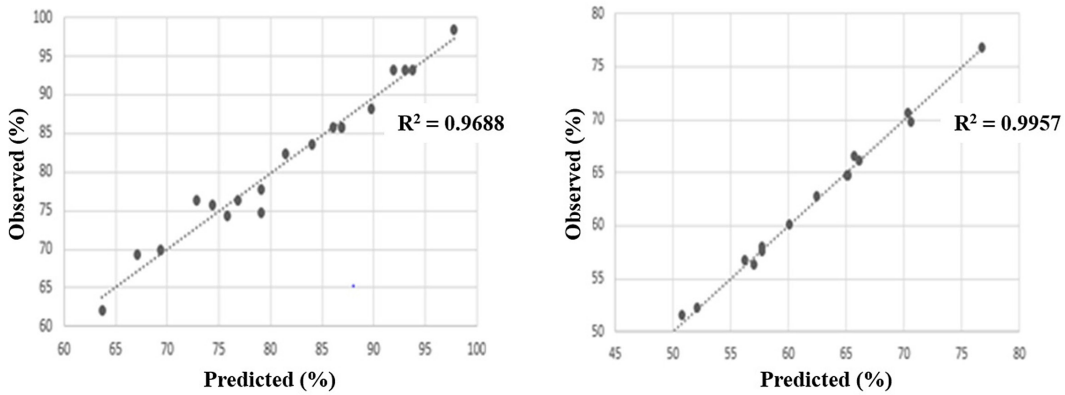

Figure 2. Experimental results versus those predicted by the models for the concentrations of cellulose (left) and lignin (right).

leading to lower cellulose yield. In our case, this would be especially relevant if we take into account that OTP-AH fibers had been previously subjected to an acid pretreatment. Regarding lignin concentration, the negative value of the coefficient c is in agreement with enrichment of cellulose at higher NaOH concentrations. Furthermore, the interactive coefficients among the three variables contributed to higher biomass delignification in the range $Tc > tT > tc$. In contrast, an unexpected slight positive influence of t, T and t^2 in lignin concentration was observed (Eqn 13).

Figure 3 illustrates the RSM curves, which were plotted at fixed c values while varying t and T. From the analysis of this figure, it can be deduced that both response variables are sensitive to the variation in NaOH concentration because for $c = 1$ the observed effects were different to those for $c = -1$ and $c = 0$. In the case of cellulose, the shape of the RSM plot is similar at the three c levels, but the effect appears to be more pronounced with increasing NaOH concentration (Fig. 3 top). It can be observed that intermediate temperature and time seem to lead to higher cellulose concentration. Nevertheless, the effects were more variable for lignin concentration (Fig. 3 bottom). At the lowest NaOH concentration (4%) an increase of the reaction temperature led to an unexpected slight increase in lignin concentration, while the effect of reaction time was practically negligible. However, higher T implied a clear decrease in lignin concentration at 8% NaOH.

By using this approach, the optimal conditions for maximum delignification and cellulose enrichment were

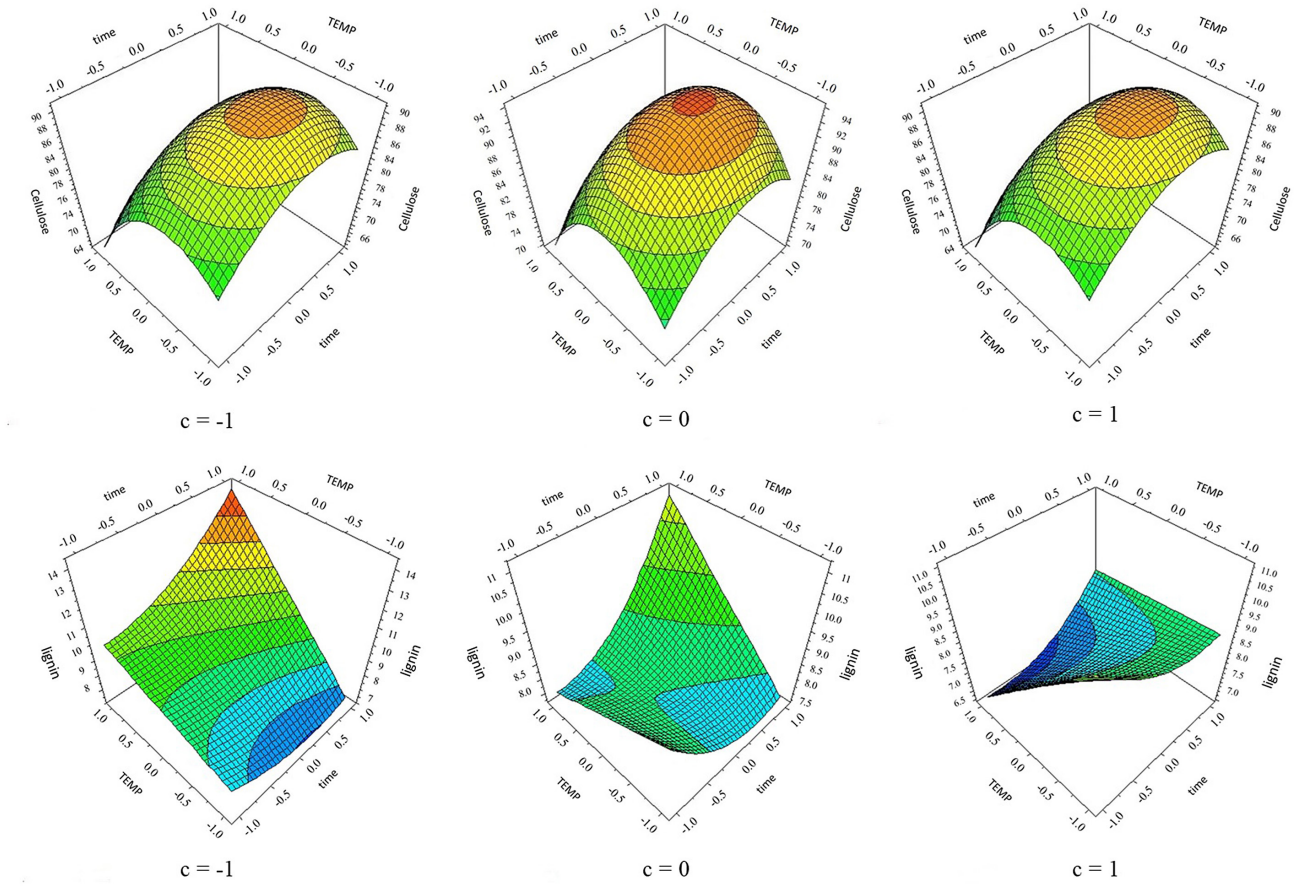

Figure 3. Response surfaces obtained from the experimental design showing the interactive effect of *t*, *T* and *c* on the concentrations of cellulose (top) and lignin (bottom) for different values of NaOH concentration (*c*): *c* = –1 (4%), *c* = 0 (6%) and *c* = 1 (8%).

Table 3. Validation of the model for the optimization of alkaline hydrolysis.

Experimental conditions			Experimental values		Predicted values	
t (min)	*T* (°C)	NaOH (%)	Cellulose (%)	Lignin (%)	Cellulose (%)	Lignin (%)
104	82.7	8	89.08	5.61	91.8	6.0

Table 4. Chemical composition of olive tree pruning samples, moisture and yield of each reaction.

Biomass fibers	Moisture (%)	Cellulose (%)	Hemicellulose (%)	Lignin (%)	Yield (%)
OTP	5.67	31.53	21.61	24.76	-
OTP-AH	7.39	63.32[†]	8.92[†]	7.78[†]	30.90[†]
OTP-BH	5.53	89.08	n.d.	5.61	60.85
OTP-BL	5.62	95.10	n.d.	5.70	89.70

n.d., not detected.
[†]Rodríguez-Liébana *et al*.[29]

identified as *t* = –0.065 (104 min), *T* = 0.772 (82.7 °C), and *c* = 1 (8% NaOH). This was confirmed by performing the alkaline hydrolysis under these conditions. As shown in Table 3, cellulose and lignin concentrations were 89.1% and 5.6% respectively. The values predicted by the quadratic equations were slightly higher than those from the experimental confirmation. More particularly, deviations of 3% and 7% with respect to the experimental result were found

for cellulose and lignin concentrations, respectively, thus verifying the validity of the model.

The OTP fibers under the optimized alkaline treatment (OTP-BH) were eventually subjected to the H_2O_2 bleaching reaction described above to obtain purified cellulose pulp (OTP-BL) with a strong whiteness (Fig. 1). The yellow-brown color of the biomass turned white after the bleaching treatment and the elimination of non-cellulosic components such as pectin, hemicellulose, and lignin.[42]

The single-step yields can be found in Table 4. Considering all the single-steps yields of the treatments (acid hydrolysis, alkaline hydrolysis, and bleaching), a global yield of 16.87% is obtained using Eqn (5). Kian *et al.* (2020)[46] reported a global yield after purification of cellulose content of 24.9% from olive pruning fibers. This process consisted of a bleaching step followed by alkaline hydrolysis, obtaining a cellulose content of 79.8 wt.%.

As shown in Table 4, the concentration of cellulose after bleaching was as high as 95.1%, whereas the concentration of lignin remained practically unaltered. However, the yield of cellulose with respect to the initial raw OTP was too low (16.9 g OTP-BL per 100 g raw OTP).

The cellulose mass balance was calculated by taking into account the yield of each stage of the process and the concentration of cellulose in the corresponding fibers. At the end of the whole process, only 51% of the cellulose originally present in OTP was retained in OTP-BL fibers (Table 5). This high cellulose loss was mainly produced during the acid pretreatment (around 38% loss) and, secondarily, after alkaline and bleaching reactions that contributed with 9% and 2% losses respectively. This is in line with the report by Candido and Gonçalves,[47] who obtained a total cellulose loss from sugarcane straw of 28% and stated that acid pretreatment (10% H_2SO_4, 100 °C, 1 h, 1:10 solid/liquid ratio) proportioned a relatively high solubilization rate of cellulose.

Fourier transform infrared spectroscopy of OTP fibers

The FTIR spectra of raw OTP and the different OTP pulps (Fig. 4) were used to examine the process of cellulose purification. Two spectral zones, in the ranges 800–1800 cm^{-1} and 2800–3600 cm^{-1}, can be clearly distinguished. From higher to lower wavenumber, the broad band in the range 3600–3000 cm^{-1} represented the stretching vibration of the different —OH groups present in cellulose, hemicellulose, lignin, and the retained water.[33,37,38,40,48] The peaks observed in the 3000–2800 cm^{-1} region are associated with the stretching vibration of C-H bonds in —CH_3, —CH_2 and —O—CH_3 groups of cellulose, hemicellulose and lignin.[37,38,49]

As observed in Fig. 4, two well-defined peaks appeared after acid pretreatment and, after the alkaline hydrolysis, the pattern changed to obtain a smooth band. The peaks at wavenumber 1600–1750 cm^{-1} are ascribed to the stretching of C═O bonds in esters and, in general, carbonyl-type groups present in lignin (ferulic and *p*-coumeric acids) and hemicellulose (acetyl and uronic esters).[38,48,50,51] Absorption in this region was therefore reduced progressively with the chemical treatments, especially after alkaline hydrolysis. Similarly, the NaOH treatment led to the disappearance of the peak at approximately 1600 cm^{-1}, which has been attributed to the aromatic C—C stretching and to the fluctuation of the —C═O stretch of conjugated *p*-substituted aryl ketones in lignin.[38,40] Since the absorption at 1500–1400 cm^{-1} and 1240–1160 cm^{-1} are associated with the stretching of C═C linkages of the aromatic rings in lignin,[48,50] and to the C–O bonds in cellulose, hemicellulose, and acetyl groups of lignin respectively,[51] lower intensity in these regions was also observed. In contrast, the peaks observed at wavelengths between 1100 and 1020 cm^{-1} (skeletal vibration of the C—O—C pyranose ring) and approximately 890 cm^{-1}, corresponding to the vibration of the glycosidic bonds between cellulose monomers,[37] were better defined with the progress of the treatment. All these findings corroborated the ability of the process to remove noncellulosic compounds, thus leading to cellulose isolation, and confirm that FTIR spectroscopy is a facile and rapid technique to monitor the main changes produced in lignocellulosic biomass after fractionation.

Table 5. Mass balance during cellulose isolation.

Biomass fibers	Cellulose (g/100 g raw OTP)	Cellulose loss (g)
OTP	31.53	–
OTP-AH	19.57	11.96
OTP-BH	16.75	2.82
OTP-BL	16.04	0.71

X-ray diffraction of OTP fibers

Unlike lignin and hemicellulose, which are purely amorphous in nature, cellulose structure contains both crystalline and amorphous phases. Hence, the evaluation of the crystalline structure of OTP samples by XRD is also a rapid method to monitor the elimination of lignin and hemicellulose. The diffractograms of raw OTP, OTP-AH, OTP-BH, and OTP-BL are shown in Fig. 5. The shape of the XRD curve of the original OTP presented a broad band with a maximum at around 22.1°, thus indicating the presence of a large quantity of amorphous components (hemicelluloses, lignin, and other nondetermined amorphous compounds). Moreover, the

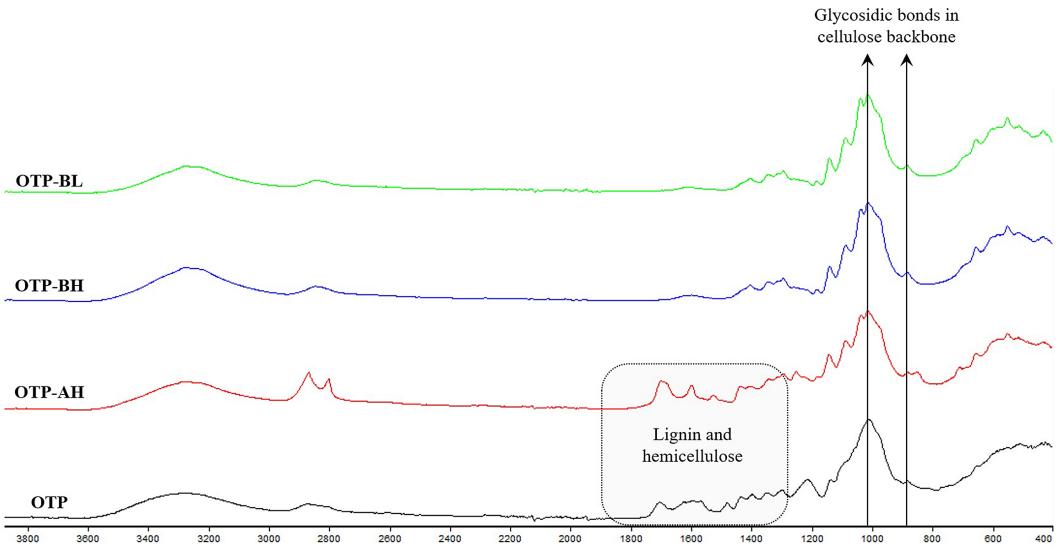

Figure 4. Fourier transform infrared spectra of raw OTP, OTP-AH, OTP-BH, and OTP-BL.

discrete peak at approximately 34.5° suggested some order along the molecular axis. With the chemical treatments, three main changes were clearly visible: an overlapped peak at $2\theta \approx 16.5°$ resulting from crystal planes with Miller indices of (1–10) and (110); the sharpening of the main crystalline peak ($2\theta \approx 22.5°$) corresponding to the (200) planes; and the intensification of the (004) peak at $2\theta \approx 34.5°$, which can be also partly due to preferred orientation of crystals in the samples.[36] This is consistent with the structure of cellulose type I,[38,40,52–54] thus confirming extensive elimination of hemicellulose and lignin already after the acid pretreatment. The occurrence of these peaks related with cellulose type I in all the samples suggested that the crystalline structure was conserved during each step of the treatment.

Table 6 includes the results of the calculated *CrI*. Raw OTP waste had a minimum value of *CrI* of 40.9%. The *CrI* values increased with the gradual enrichment in cellulose. After acid pretreatment, *CrI* increased substantially to 63.9% because most of the amorphous material was removed at this stage. A further increase was achieved after alkaline hydrolysis (*CrI* OTP-BH = 71.1%), whereas the crystallinity was practically not modified during bleaching.

Thermogravimetric analysis of OTP fibers

The heat stability of raw OTP and after each stage of the treatment was analyzed by thermogravimetric analysis-derivative thermogravimetry (TGA-DTG) under pyrolysis conditions (Fig. 6). An initial weight loss from room temperature up to 150 °C was observed in all the samples, with values of 8.9% for raw OTP, 6.9% for OTP-AH, 5.5% for OTP-BH, and 4.4% for OTP-BL. Some authors have exclusively related this initial weight loss to the desorption and evaporation of water[38,40–50] and with the hydrophilic character of lignocellulose.[36] However, it is

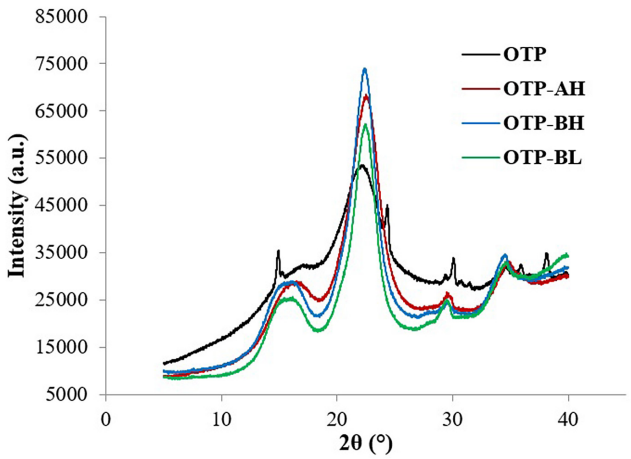

Figure 5. X-ray diffraction patterns of raw OTP, OTP-AH, OTP-BH, and OTP-BL.

Table 6. X-ray diffraction analysis of olive tree pruning samples.

Biomass fibers	Crystalline fraction		Amorphous fraction		*CrI* (%)
	2θ (°)	I_{200}	2θ (°)	I_{am}	
OTP	22.1	53577	18.0	31651	40.9
OTP-AH	22.5	68570	18.4	24737	63.9
OTP-BH	22.4	74052	18.5	21430	71.1
OTP-BL	22.5	62277	18.3	18317	70.6

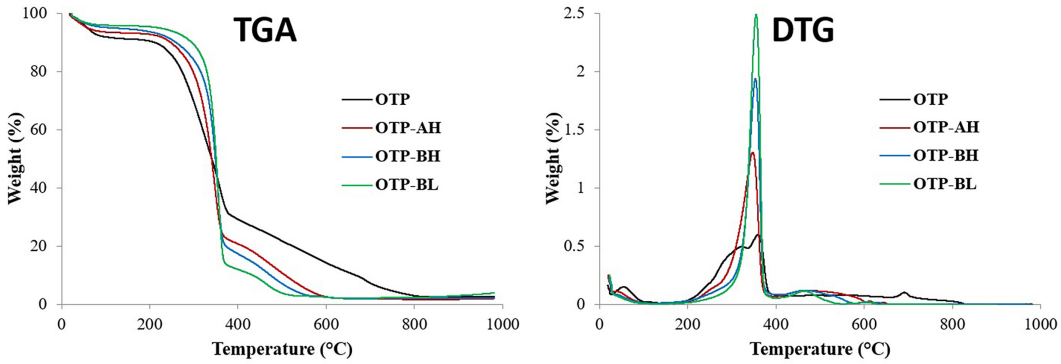

Figure 6. Thermogravimetric analysis (left) and derivative thermogravimetry (DTG) (right) curves of raw OTP, OTP-AH, OTP-BH and OTP-BL.

important to consider the contribution of other volatiles, such as extractives and low molecular-weight compounds, particularly in untreated biomass.[27,55] Besides this initial event, the degradation of all the OTP samples started at approximately 200 °C. The thermogram of raw OTP showed a broad band extending to almost 450 °C with a discrete peak at 359 °C. This pattern is typical of lignocellulosic materials[38,50,55] and is due to the simultaneous decomposition of their major components, namely hemicellulose, cellulose and lignin in this region of the thermogram. The shape and height of the pattern in DTG curves is therefore dependent on the specific composition of the fibers. With the removal of hemicellulose and lignin, the degradation in this temperature interval was ascribed mostly to cellulose, so the peak became sharper as the treatment progressed – that is, with increased concentration of cellulose. Lignin is more thermally stable at higher temperatures. Yang *et al.*[56] stated that lignin has a slow thermal degradation kinetic and may decompose from 160 °C up to 900 °C. Lignin was therefore mainly responsible for the weight loss observed at temperatures higher than 450 °C.

The DTG plots revealed that the progress in the chemical treatment implied a slight enhancement in the thermal stability of OTP fibers, because the maximum degradation temperature was 347 °C for OTP-AH, 353 °C for OTP-BH, and 355 °C for the bleached cellulose pulp (OTP-BL).

Effect of reaction time on the acetylation of the extracted cellulose

Fourier transform infrared spectroscopy

Following extraction, the cellulose pulp (OTP-BL) was used as feedstock for the synthesis of cellulose acetate (OTP-CA). As shown in the FTIR spectra (Fig. 7), successful acetylation was already observed after 1 h of reaction. The most evident confirmation is that three peaks characteristic of the acetyl group appeared in the spectra of acetylated samples. From lower to higher wavelength: (i) stretching of C—O bond (~1220 cm^{-1}); (ii) stretching of C—H bond in acetyl CH_3 (~1370 cm^{-1}); and (iii) stretching of C═O bond (~1740 cm^{-1}).[27,33,55,57,58] In addition, in comparison with the spectrum of OTP-BL the absorption at 3600–3000 cm^{-1} corresponding to the stretching vibration of —OH bonds disappeared or was practically negligible in all the spectra of the acetate samples, thus suggesting a high level of acetylation even for the shortest reaction time.[37,47,53,55,57,58]

The extent of acetylation of OTP-CA1-6 samples was assessed by examination of $R_{FT\text{-}IR}$ as described above. Figure 8 displays the graphical representation of $R_{FT\text{-}IR}$ versus reaction time. As shown, $R_{FT\text{-}IR}$ increased from 0.62 (t = 1 h) to 0.71 (t = 4 h), and then leveled to remain practically unchanged up to t = 6 h. The values of $DS_{FT\text{-}IR}$ calculated from $R_{FT\text{-}IR}$ (Eqn 10) oscillated in the range 2.50–2.62, so cellulose diacetate was synthesized in all the cases. This relatively high acetylation extent has been attributed previously to the swelling of the fibers and increased accessibility of cellulose —OH groups after alkaline hydrolysis.[47] As lignin competes with cellulose for the acylation reagent,[47,57] our results are also consistent with the extensive removal of lignin discussed above.

Our data are similar to those previously reported.[23,31,53,58–60] In our previous work, we reported that the extent of acetylation of cellulose extracted from brewer's spent grain peaked at 2 h and then remained constant up to 5 h.[58] The extent of acetylation of bacterial cellulose has been reported to increase until 4 h, and then kept practically constant up to 16 h.[53] In another study, Adebajo and Frost[31] reported that the extent of acetylation of raw cotton and cotton fabrics increased from 1 to 3 h and then, after a slight reduction, increased again in the range 4–10 h. The acetylation of cornhusk cellulose by

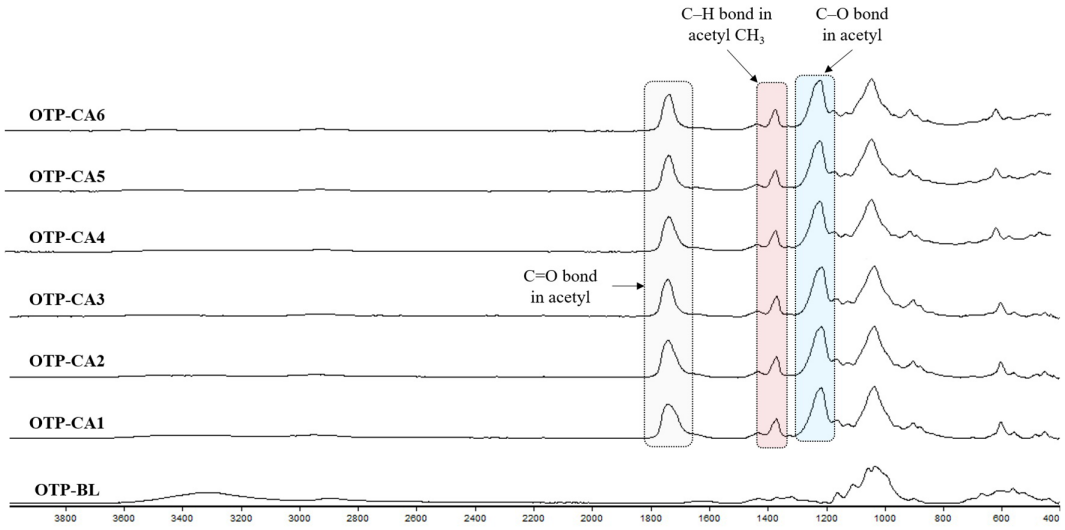

Figure 7. Fourier transform infrared spectra of the cellulose acetates synthesized at different reaction times (1–6 h). Comparison with the isolated cellulose pulp (OTP-BL).

a homogeneous mechanism with ionic liquid reached a maximum at 3 h, and then leveled to obtain a DS of 2.63 at 8 h.[59] By using I_2 as catalyst instead of H_2SO_4, acetylation of cellulose from different rice by-products either gradually increased from 1 to 5 h[23] or reached a maximum after 2 h.[60] In contrast, other authors have reported that higher reaction times were required to optimize cellulose acetylation. For instance, maximum acetylation extent of cotton linters at 80 °C has been found to be reached at 24 h.[33] In a different work, El Boustani *et al.*[57] studied the acetylation of different lignocellulosic fibers from 30 min to 24 h in a solvent-free system at room temperature and static conditions. They concluded that the extent of acetylation of the fibers increased with reaction time without reaching a maximum, and that acetylation was more significant for kraft pulp followed by thermomechanical pulp and flax fibers. More recently, Andrade-Alves *et al.*[55] reported that maximum acetylation of sorghum straw cellulose at 25 °C occurred after 16 h.

This variability is likely a consequence of the different experimental conditions used (acetylation time, temperature, catalyst, mechanism, etc.) but also of the different lignocellulosic sources used and on the processes followed for the isolation of cellulose. It has been postulated that hydrolysis of the synthesized cellulose acetate and degradation of the cellulose structure may occur during the acetylation of cellulose, especially at reaction times exceeding the maximum acetylation extent.[31] We obtained a maximum acetylation extent of OTP-BL at 4 h and, as $R_{FT\text{-}IR}$ remained constant, these side reactions likely occurred at longer times.

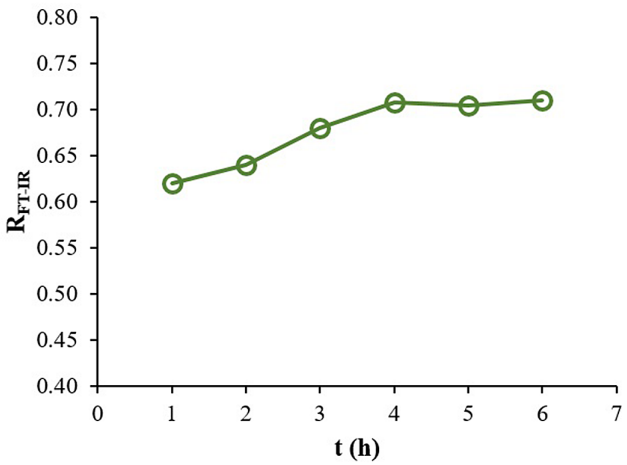

Figure 8. Effect of reaction time on the acetylation extent ($R_{FT\text{-}IR}$).

X-ray diffraction

In the typical heterogeneous mechanism, acetylation of cellulose starts with a suspension of the fibers in the acetic acid medium. During the reaction, the amorphous regions of the cellulose fibers are acetylated first, and then the crystallites are attacked from the exterior surface to their centers. As the fibers are acetylated, the synthesized product is dissolved in the reaction medium, thus impairing the integrity of the crystalline structure.[61] As the final product is dissolved in the medium, some authors have referred to this mechanism as *quasi*-homogeneous.[62]

Acetylation of cellulose leads to a rearrangement of the cellulose chains due to the fact that —OH groups are

substituted by acetyl moieties, the latter occupying greater volume in the structure. This produces a disruption in the H—bonding network of the cellulose skeleton, which causes the cleavage of the microfibrillar structure and the broadening of the interlayer space of the crystalline surface.[53,55,63] As the crystallinity of cellulose acetate has been associated with higher acetylation extent,[53,64] no significant differences were observed in the XRD plots of the different OTP-CA samples (Fig. 9), as the acetylation extent was similar (Fig. 8). The OTP-CA samples presented the typical morphology of semi-crystalline materials in which crystalline and noncrystallinity portions are mixed.[65]

The sharp peak displayed in Fig. 5 by OTP-BL fibers was transformed into a broad band that maintained the peak at approximately $2\theta = 22–22.5°$ after acetylation, which is an indication of the dominance of amorphous structures in the polymer. In line with Andrade-Alves *et al.*[55], both the crystalline peak at $2\theta = 9°$ and the shoulder (or discrete peak) at $2\theta = 18°$ confirmed that the synthesized products corresponded to cellulose diacetate.

Thermogravimetric analysis

Figure 10 shows that the thermal stability of the OTP-CA samples was enhanced with increasing acetylation time. An initial weight loss between room temperature and 150 °C was displayed in all the cases. This weight loss peaked at 62 °C for OTP-CA2, 54 °C for OTP-CA, 50 °C for OTP-CA5, and 51 °C for OTP-CA6, and represented 6.4%, 6.1%, 3.6% and 3.2% losses respectively. Traditionally, it has been assigned to the evaporation and desorption of water.[23,27,28,66] It is therefore suggested that, although all OTP-CA samples had similar DS values, higher acetylation time induced lower ability to retain moisture. However, this initial weight loss could be also due to the inefficient removal of acetic acid and/or acetic anhydride during the washing and drying steps after acetylation.[55]

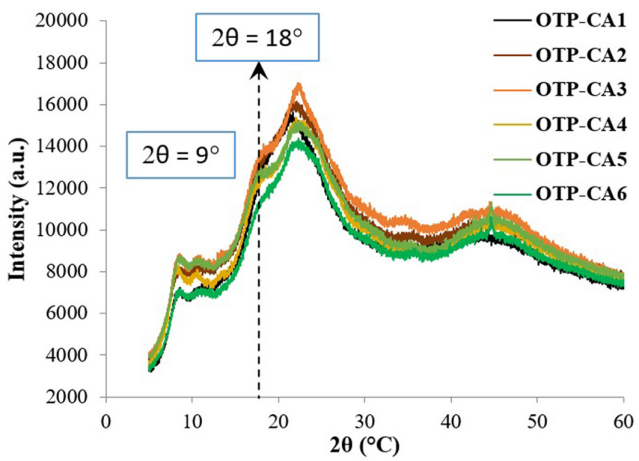

Figure 9. X-ray diffraction (XRD) patterns of the cellulose acetates synthesized at different reaction times (1–6 h).

The thermal stability from 150 °C evolved from a multistep decomposition pattern at shorter reaction times to a single sharp peak at longer times. The DTG curve of OTP-CA2 showed a band up to approximately 300 °C with a peak at 285 °C, which represented 46.3% loss. In OTP-CA4 this band amounted for 32.4% weight loss and was divided into a main peak at 199 °C followed by additional small peaks at 234, 253 and 264 °C. This behavior has been also observed for the acetylation of cellulose from brewer's spent grains,[58] and, according to Barud *et al.*,[53] is related to the degradation of preacetylated and partly hydrolyzed polymer chains as a consequence of nonhomogeneous distribution of acetyl groups in the polymer backbone. Degradation of OTP-CA5 and OTP-CA6 in this temperature interval was significantly lower as their weight loss between 150 and 300 °C was 10.6% and 5.0% respectively, thus suggesting more homogeneous distribution of acetyls.

All of the samples exhibited a degradation event that was broader, less intense, and shifted to lower temperatures for short reaction times. This is associated with deacetylation, depolymerization, and pyrolysis of the cellulose backbone that occurred up to approximately 400 °C. This event peaked at 347 °C for OTP-CA2, 345 °C for OTP-CA4, 362 °C for OTP-CA5, and 365 °C for OTP-CA6, and represented 24.3%, 41.0%, 66.6%, and 73.2% weight loss respectively. As the maximum degradation temperature of the OTP-BL pulp was 355 °C, it could indicate that 6 h would preferably be required to obtain cellulose acetate with higher thermal stability. The thermograms were quite similar from 400 °C to the end of the pyrolysis, with an amount of carbonized mass that progressively decreased from 16.0% for OTP-CA2 to 12.3% for OTP-CA6.

Conclusions

Noncellulosic components were removed from OTP fibers effectively. During alkaline hydrolysis, higher temperatures seemed to damage cellulose, whereas the interactions among the three independent variables contributed to greater removal of lignin from OTP fibers. Optimized delignification conditions were fixed at $t = 104$ min, $T = 82.7$ °C, and $c = 8\%$ NaOH. After bleaching, a pulp with 95% cellulose, 71% *CrI* and 355 °C maximum degradation temperature was produced. However, around 50% of the cellulose was removed during the whole chemical treatment, with acid pretreatment, alkaline hydrolysis and bleaching being responsible for 77.2%, 18.2%, and 4.6% of the elimination respectively.

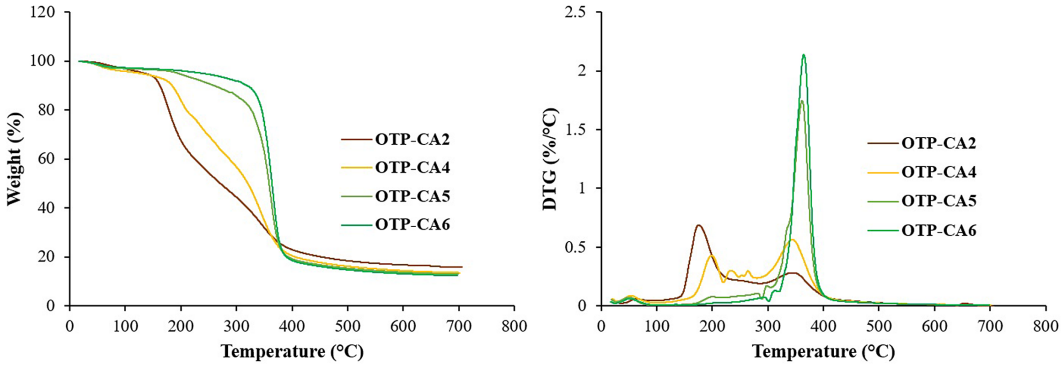

Figure 10. Thermogravimetric analysis (TGA) (left) and derivative thermogravimetry (DTG) (right) curves of OTP-CA2, OTP-CA4, OTP-CA5, and OTP-CA6.

Regarding acetylation, the analysis of the infrared spectra indicated that the relatively high extent of the acetylation of the cellulose was already achieved at reaction times as short as 1 h, and then it was practically unchanged for the time interval assayed. As a result, the synthesized cellulose acetates had degrees of substitution that varied in a narrow range (2.50–2.62). The large extent of acetylation is also associated with the high crystallinity of cellulose acetate, which influences the thermal behavior of the samples. The thermal analysis revealed that higher acetylation time led to products with improved thermal stability. Short reaction times (up to 4 h) yielded cellulose diacetates with multistep degradation patterns, the thermograms of OTP-CA5 and OTP-CA6 displayed a single peak between 300 and 400 °C with a maximum above 360 °C related to deacetylation, depolymerization, and pyrolitic decomposition of the polymer. We may therefore conclude that preferably 6 h was needed to obtain a cellulose diacetate with uniform distribution of acetyl groups and adequate thermal stability for further processing.

The possible industrial applications of the CA obtained through this procedure could be those of a commercial CA with similar characteristics obtained from conventional nonwaste sources – that is, its processing using different conventional polymer transformation technologies (such as injection and extrusion) to obtain plastic products. Of all of them, the CA obtained in this work was developed with the aim of using it in future works for the manufacture of biofilms devoted to food packaging and separation membrane applications.

The production of CA using this approach presents some advantages from different perspectives. It provides environmental advantages by establishing a new route for obtaining CA from agricultural waste and an alternative to burning (avoiding associated emissions) or the dispersion of chopped OTP in the soil (without added value). The economic advantage is that it constitutes a new way of revaluating OTP that allows polymers to be obtained that have high added value and are in great demand in the market. There are social advantages, given that it has strong potential to generate new business models, based on the principles of the circular economy, in agricultural areas of southern Spain where olive grove cultivation is concentrated and which are, in many cases, at high risk of depopulation.

Abbreviations

AIL	acid insoluble lignin (%)
ATR	attenuated total reflectance
c	NaOH concentration
CrI	crystallinity index (%)
$DS_{FT\text{-}IR}$	degree of substitution ($DS_{FT\text{-}IR}$) of OTP-CA
DTG	derivative thermogravimetry
FCCD	face-centered central composite design
HPLC	high-performance liquid chromatography
I_{200}	maximum intensity of the (*200*) lattice diffraction peak corresponding to both amorphous and crystalline phases
I_{am}	intensity scattered by the amorphous part
m	weight of the unhydrolyzed solid before incineration
mo	weights of the sample before drying (g)
m_{105}	weights of the sample after drying (g)
m_{600}	weight of the unhydrolyzed solid after incineration.
m_{OTP}	weight (g) of raw olive tree pruning
$m_{OTP\text{-}AH}$	weight (g) of olive tree pruning after acid treatment
$m_{OTP\text{-}BH}$	weight (g) of olive tree pruning after acid treatment and alkaline hydrolysis
$m_{OTP\text{-}BL}$	weight (g) of olive tree pruning after acid treatment, alkaline hydrolysis and bleaching

OTP	olive tree pruning
OTP-AH	olive tree pruning fibers after the acid treatment
OTP-BH	olive tree pruning fibers after the acid treatment and alkaline hydrolysis
OTP-BL	olive tree pruning fibers bleached after acid and basic treatments
OTP-CA	cellulose acetate obtained from olive tree pruning
OTP-CAx	cellulose acetate obtained from olive tree pruning after x hours of acetylation reaction ($x = 1$ to 6)
$R_{FT\text{-}IR}$	acetylation extent index
RSM	response surface methodology
t	reaction time
T	temperature
TGA	thermogravimetric analysis
WG_{FT-IR}	weight per percent gain
x_i	independent variable i
x_j	independent variable j
XRD	X-ray diffraction
Y	Y is the specific response function,
Y_{AH}	yield of acid pretreatment
Y_{BH}	yield of alkaline hydrolysis
Y_{BL}	yield of bleaching reaction
β_0	constant
β_i	linear, quadratic and interactive coefficient i
β_{ii}	linear, quadratic and interactive coefficient ii
β_{ij}	linear, quadratic and interactive coefficient ij

Acknowledgements

This study has been conducted within the framework of the BIONANOCEL project funded by the Regional Government of Andalusia through FEDER funds (PY18-RE-0016). The authors thank the technical and human support provided by Centro de Instrumentación Científico-Técnica (CICT) – Universidad de Jaén (UJA, MICINN, Junta de Andalucía, FEDER), and by M. José de la Mata (Autonomous University of Madrid).

References

1. Debnath A, Sengupta A, Saha A and Das A, Utilization of agro waste for beneficial product formulation. *J Exp Biol Agric Sci* **10**(1):157–170 (2022).
2. Tsoraeva E, Bekmurzov A, Kozyrev S, Khoziev A and Kozyrev A, Environmental issues of agriculture as a consequence of the intensification of the development of agricultural industry. *E3S Web Conf* **215**:02003 (2020).
3. Turmel MS, Speratti A, Baudron F, Verhulst N and Govaerts B, Crop residue management and soil health: a systems analysis. *Agr Syst* **134**:6–16 (2015).
4. Anwar Z, Gulfraz M and Irshad M, Agro-industrial lignocellulosic biomass a key to unlock the future of bio-energy: a review. *J Radiat Res Appl Sci* **7**(2):163–173 (2014).
5. Yekta R, Abedi-Firoozjah R and Azimi SS, Application of cellulose and cellulose derivatives in smart/intelligent bio-based food packaging. *Cellulose* **30**:9925–9953 (2023).
6. Sharma R, Nath PC, Mohanta YK, Bhunia B, Mishra B, Sharma M *et al*., Recent advances in cellulose-based sustainable materials for wastewater treatment: an overview. *Int J Biological Macromol* **256**(2):128517 (2024).
7. Ling-Zhi H, Ming-Guo M, Xing-Xiang J, Sun-Eun C and Chuanling S, Recent developments and applications of hemicellulose from wheat straw: a review. *Front Bioeng Biotechnol* **9** (2021) 690773.
8. Sganzerla WG, da Silva MF, Zabot GL, Goldbeck R, Mussatto SI and Forster-Carneiro T, Techno-economic assessment of subcritical water hydrolysis of brewer's spent grains to recover xylo-oligosaccharides. *J Supercrit Fluids* **196**:105895 (2023).
9. Mussato SI, Brewer's spent grain: a valuable feedstock for industrial applications. *J Sci Food Agric* **94**:1264–1275 (2014).
10. Feghali E, Van de Pas DJ, Kirk M and Torr KM, Toward bio-based epoxy thermoset polymers from depolymerized native lignins produced at the pilot scale. *Biomacromolecules* **21**(4):1548–1559 (2020).
11. Quinsaat JEQ, Falireas PG, Feghali E, Torr KM, Vanbroekhoven K, Eevers W *et al*., Depolymerised lignin oil: a promising building block towards thermoplasticity in polyurethanes. *Ind Crops Prod* **194**:116305 (2023).
12. Zikeli F, Vinciguerra V, Sennato S, Mugnozza GS and Romagnoli M, Preparation of lignin nanoparticles with entrapped essential oil as a bio-based biocide delivery system. *ACS Omega* **5**(1):358–368 (2020).
13. Robinson AJ, Abdelaziz OY, Hulteberg CP, Koutinas A, Triantafyllidis KS, Barletta D *et al*., Techno-economic optimization of a process superstructure for lignin valorization. *Bioresour Technol* **364**:28004 (2022).
14. Chen Y, Stevens MA, Zhu Y, Holmes J and Xu H, Understanding of alkaline pretreatment parameters for corn stover enzymatic saccharification. *Biotechnol Biofuels* **6**(1):8 (2013).
15. Mateo S, Peinado S, Morillas-Gutiérrez F, La Rubia MD and Moya AJ, Nanocellulose from agricultural wastes: products and applications – a review. *Processes* **9**(9):1594 (2021).
16. Shipovskaya AB, Rogacheva SM and Malinkina ON, Method of obtaining cellulose diacetate with a pregiven chiral structure for highly efficient materials. *Cellulose* **27**(16):9285–9298 (2020).
17. Abdellah Ali SF, William LA and Fadl EA, Cellulose acetate, cellulose acetate propionate and cellulose acetate butyrate membranes for water desalination applications. *Cellulose* **27**(16):9525–9543 (2020).
18. Abdelhameed RM, Abdel-Gawad H and Emam HE, Macroporous Cu-MOF@cellulose acetate membrane serviceable in selective removal of dimethoate pesticide from wastewater. *J Environ Chem Eng* **9**(2):105121 (2021).
19. Idress H, Zaidi SZJ, Sabir A, Shafiq M, Khan RU, Harito C *et al*., Cellulose acetate based complexation-NF membranes for the removal of Pb(II) from waste water. *Sci Rep* **11**(1):1806 (2021).
20. Ribeiro SD, Meneguin AB, Barud HS, Silva JM, Oliveira RL, Asunção RMN *et al*., Synthesis and characterization of cellulose acetate from cellophane industry residues. Application as acetaminophen controlled-release membranes. *J Therm Anal Calorim* **147**(13):7265–7275 (2022).

21. Paiva MTP, da Silva JBMD, Brisola J, de Carvalho GM and Mali S, Cellulose acetate from lignocellulosic residues: an eco-friendly approach based on a hydrothermal process. *Int J Biol Macromol* **243**:125237 (2023).
22. Sodeinde KO, Ojo AM, Olusanya SO, Ayanda OS, Adeoye AO, Dada TM *et al*., Cellulose isolated from Delonixregia pods: characterisation and application in the encapsulation of vitamin A. *Ind Crops Prod* **160**:113138 (2021).
23. Das AM, Ali AA and Hazarika MP, Synthesis and characterization of cellulose acetate from rice husk: eco-friendly condition. *Carbohydr Polym* **112**:342–349 (2014).
24. Cheng HN, Dowd MK, Selling GW and Biswas A, Synthesis of cellulose acetate from cotton byproducts. *Carbohydr Polym* **80**(2):449–452 (2010).
25. Amaral HR, Cipriano DF, Santos MS, Shettino MA, Ferreti JVT, Meirelles CS *et al*., Production of high-purity cellulose, cellulose acetate and cellulose-silica composite from babassu coconut shells. *Carbohydr Polym* **210**:127–134 (2019).
26. Cerqueira DA, Filho GR, Carvalho RDA and Valente AJM, Caracterização de acetato de celulose obtido a partir do bagaço de cana-de-açúcar por ^{1}H-RMN. *Polimeros* **20**(2):85–91 (2010).
27. Candido RG, Godoy GG and Gonçalves A, Characterization and application of cellulose acetate synthesized from sugarcane bagasse. *Carbohydr Polym* **167**:280–289 (2017).
28. Wan Daud WR and Djuned FM, Cellulose acetate from oil palm empty fruit bunch via a one step heterogeneous acetylation. *Carbohydr Polym* **132**:252–260 (2015).
29. Rodríguez-Liébana JA, Navas-Martos FJ, Jurado-Contreras S, Morillas-Gutiérrez F, Mateo S, Moya AJ *et al*., Manufacture and characterisation of polylactic acid biocomposites with high-purity cellulose isolated from olive pruning waste. *J Reinf Plast Compos* (2023).
30. Sluiter A, Hames B, Ruiz R, Scarlata C, Sluiter J, Templeton D *et al*., *Determination of Structural Carbohydrates and Lignin in Biomass*. National Renewable Energy Laboratory; Laboratory Analytical Procedure (LAP), (2008). Denver, CO.
31. Adebajo MO and Frost RL, Acetylation of raw cotton for oil spill cleanup application: an FTIR and ^{13}C MAS NMR spectroscopic investigation. *Spectrochim Acta A Mol Biomol Spectrosc* **60**(10):2315–2321 (2004).
32. Nemr AE, Ragab S and Sikaily AE, Rapid synthesis of cellulose triacetate from cotton cellulose and its effect on specific surface area and particle size distribution. *Iran Polym J* **26**(4):261–272 (2017).
33. Fei P, Liao L, Cheng B and Song J, Quantitative analysis of cellulose acetate with a high degree of substitution by FTIR and its application. *Anal Methods* **9**(43):6194–6201 (2017).
34. Li W, Cai G and Zhang P, A simple and rapid Fourier transform infrared method for the determination of the degree of acetyl substitution of cellulose nanocrystals. *J Mater Sci* **54**(10):8047–8056 (2019).
35. Segal L, Creely JJ, Martin AE and Conrad CM, An empirical method for estimating the degree of crystallinity of native cellulose using the X-ray diffractometer. *Text Res J* **29**(10):786–794 (1959).
36. Johar N, Ahmad I and Dufresne A, Extraction, preparation and characterization of cellulose fibres and nanocrystals from rice husk. *Ind Crops Prod* **37**(1):93–99 (2012).
37. Kassab Z, Abdellaoui Y, Hamid Salim M, Bouhfid R, El Kacem QA and El Achaby M, Micro- and nano-celluloses derived from hemp stalks and their effect as polymer reinforcing materials. *Carbohydr Polym* **245**:116506 (2020).
38. Raza M, Abu-Jdayil B, Banat F and Al-Marzouqi AH, Isolation and characterization of cellulose nanocrystals from date palm waste. *ACS Omega* **7**(29):25366–25379 (2022).
39. Lan J, Chen J, Zhu R, Lin C, Ma X and Cao S, Antibacterial and antiviral chitosan oligosaccharide modified cellulosic fibers with durability against washing and long-acting activity. *Int J Biol Macromol* **231**:123587 (2023).
40. Rubiyah MH, Melethil K, Varghese S, Kurian M, Babu S, Jojo L *et al*., Isolation and characterization of cellulose nanofibrils from agro-biomass of Jackfruit (*Artocarpus heterophyllus*) rind, using a soft and benign acid hydrolysis. *Carbohydr Polym Technol Appl* **6**:100374 (2023).
41. Rowell RM, Opportunities for lignocellulosic materials and composites, in *Emerging Technologies for Materials and Chemicals from Biomass*, Vol. **4**, pp. 12–27 (1992). Washington, DC.
42. Sung SH, Chang Y and Han J, Development of polylactic acid nanocomposite films reinforced with cellulose nanocrystals derived from coffee silverskin. *Carbohydr Polym* **169**:495–503 (2017).
43. Hakkou M, Pétrissans M, Zoulalian A and Gérardin P, Investigation of wood wettability changes during heat treatment on the basis of chemical analysis. *Polym Degrad Stabil* **89**(1):1–5 (2005).
44. Bilal M, Asgher M, Iqbal HM, Hu H and Zhang X, Biotransformation of lignocellulosic materials into value-added products – a review. *Int J Biol Macromol* **98**:447–458 (2017).
45. Melikoğlu AY, Bilek SE and Cesur S, Optimum alkaline treatment parameters for the extraction of cellulose and production of cellulose nanocrystals from apple pomace. *Carbohydr Polym* **215**:330–337 (2019).
46. Kian LK, Saba N, Jawaid M, Alothman OY and Fouad H, Properties and characteristics of nanocrystalline cellulose isolated from olive fiber. *Carbohydr Polym* **241**:116423 (2020).
47. Candido RG and Gonçalves AR, Synthesis of cellulose acetate and carboxymethylcellulose from sugarcane straw. *Carbohydr Polym* **152**:679–686 (2016).
48. Zhou L, He H, Jiang C, Ma L and Yu P, Cellulose nanocrystals from cotton stalk for reinforcement of poly(vinyl alcohol) composites. *Cellul Chem Technol* **51**(1–2):109–119 (2017).
49. Sun XF, Jing Z, Fowler P, Wu Y and Rajaratnam M, Structural characterization and isolation of lignin and hemicelluloses from barley straw. *Ind Crops Prod* **33**(3):588–598 (2011).
50. Dos Santos DM, De Lacerda BA, Ascheri DPR, Signini R and De Aquino GLB, Microwave-assisted carboxymethylation of cellulose extracted from brewer's spent grain. *Carbohydr Polym* **131**:125–133 (2015).
51. Elyamine AM, Moussa MG, Afzal J, Rana MS, Imran M, Zhao X *et al*., Modified rice straw enhanced cadmium (II) immobilization in soil and promoted the degradation of phenanthrene in co-contaminated soil. *Int J Mol Sci* **20**:2189 (2019).
52. French AD, Idealized powder diffraction patterns for cellulose polymorphs. *Cellulose* **21**(2):885–896 (2014).
53. Barud HS, de Araújo Júnior AM, Santos DB, de Assunção RMN, Meireles CS, Cerqueira DA *et al*., Thermal behavior of cellulose acetate produced from homogeneous acetylation of bacterial cellulose. *Thermochim Acta* **471**(1–2):61–69 (2008).
54. French AD and Cintrón MS, Cellulose polymorphy, crystallite size, and the Segal Crystallinity Index. *Cellulose* **20**(1):583–588 (2013).

55. Andrade JA, Lisboa dos Santos MD, Morais CC, Ramirez JL, Signini R, dos Santos DM *et al*., Sorghum straw: pulping and bleaching process optimization and synthesis of cellulose acetate. *Int J Biol Macromol* **135**:877–886 (2019).
56. Yang H, Yan R, Chen H, Lee DH and Zheng C, Characteristics of hemicellulose, cellulose and lignin pyrolysis. *Fuel* **86**(12–13):1781–1788 (2007).
57. El Boustani M, Brouillette F, Lebrun G and Belfkira A, Solvent-free acetylation of lignocellulosic fibers at room temperature: effect on fiber structure and surface properties. *J Appl Polym Sci* **132**(29):42247 (2015).
58. Camacho-Núñez L, Jurado-Contreras S, La Rubia MD, Navas-Martos FJ and Rodríguez-Liébana JA, Cellulose-based upcycling of brewer's spent grains: extraction and acetylation. *J Polym Environ* (2023).
59. Cao Y, Wu J, Meng T, Zhang J, He J and Li H, Acetone-soluble cellulose acetates prepared by one-step homogeneous acetylation of cornhusk cellulose in an ionic liquid 1-allyl-3-methylimidazolium chloride (AmimCl). *Carbohydr Polym* **69**(4):665–672 (2007).
60. Umaningrum D, Astuti MD, Nurmasari R, Hasanuddin H, Mulyasuryani A and Mardiana D, Variation of iodine mass and acetylation time on cellulose acetate synthesis from rice straw. *Indo J Chem Res* **8**(3):228–233 (2021).
61. Sassi JF and Chanzy H, Ultrastructural aspects of the acetylation of cellulose. *Cellulose* **2**(2):111–127 (1995).
62. Ciolacu D, Olaru L, Suflet D and Olaru N, Cellulose esters – from traditional chemistry to modern approaches and applications, in *Pulp Production and Processing: From Papermaking to High-Tech Products*, ed. by Popa VI. Smithers Rapra Technology, pp. 253–299 (2013). Shrewsbury, Shrposhire, UK.
63. Ching TW, Haritos V and Tanksale A, Ultrasound-assisted conversion of cellulose into hydrogel and functional carbon material. *Cellulose* **25**(4):2626–2645 (2018).
64. de Freitas RRM, Senna AM and Botaro VR, Influence of degree of substitution on termal dynamic mechanical and physicochemical properties of cellulose acetate. *Ind Crops Prod* **109**:452–458 (2017).
65. Jiang L, Huang X, Tian C, Zhong Y, Yan M, Miao C *et al*., Preparation and characterization of porous cellulose acetate nanofiber hydrogels. *Gels* **9**(6):484 (2023).
66. Rodrigues Filho G, Monteiro DS, Meireles CS, de Assunção RM, Cerqueira DA, Barud HS *et al*., Synthesis and characterization of cellulose acetate produced from recycled newspaper. *Carbohydr Polym* **73**(1):74–82 (2008).

José Antonio Rodríguez-Liébana

José Antonio Rodríguez-Liébana has been a project manager and research scientist at Andaltec I+D+I, Plastic Technological Center since the end of 2017. He specializes in polymer chemistry, functionalization, characterization, and application. He has recently participated as either team member or principal researcher in projects devoted to the treatment, conversion, and incorporation of lignocellulosic biomass into biobased products, application in polymers and plastics, and to the recycling of plastic waste.

Esther Robles-Solano

Esther Robles-Solano is a predoctoral researcher at the Institute of Materials Sciences of Seville (CSIC-University of Seville). She carries out research on 'thermochemical materials for energy storage improved through microstructural control'. She graduated in chemistry from the University of Jaén and has a double master's degree in biotechnology and biomedicine. She has collaborated in research at the University of Jaén related to the use of biomass from olive tree prunings for the synthesis of polymeric materials.

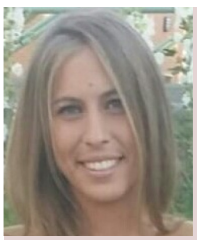

Sofia Jurado-Contreras

Sofia Jurado-Contreras is a mechanical engineer. She has a master's degree in industrial engineering and is a PhD student specializing in polymeric composite materials. She is also an R&D project manager. She has participated in several research projects on waste valorization for the development of composite materials.

Francisca Morillas-Gutiérrez

Francisca Morillas-Gutiérrez graduated in chemistry from the University of Jaén and has a master's degree in food safety. She has collaborated in research at the University of Jaén related to the use of biomass from olive tree pruning for the synthesis of polymeric materials.

Alberto J. Moya

Alberto J. Moya, is a chemical engineer with a doctorate. He is a full university professor and a member of the Institute of Research on Olive and Olive Oils (INUO) in the University of Jaén, Spain. His research specializes in the use of lignocellulosic materials from agricultural residues. He has co-authored books and research papers on science education and bioenergy products and has carried out research in Italy and Brazil.

Soledad Mateo

Soledad Mateo is a full university professor and member of the Institute of Research on Olive and Olive Oils (INUO) in the University of Jaén, Spain. Her research specializes in the utilization of lignocellulosic materials from agricultural wastes. She has co-authored books and research papers on science education and bioenergy products, and she has collaborated with researchers from other countries such as Italy and Brazil.

Francisco Javier Navas-Martos

Francisco Javier Navas-Martos has an MSc in chemistry, an MEng in chemical engineering, and a PhD in polymer technology. He is head of the R&D department. His main research works specialized in polymer science and technology, valorization of both industrial and agricultural waste, sustainable air conditioning systems, laser welding, and life cycle analysis.

M. Dolores La Rubia

M. Dolores La Rubia has an MSc in chemistry, an MSc in the science and technology of polymers, and a PhD in chemical engineering. She is currently a full professor at the University of Jaén where she develops research and conducts research projects into polymer composites, the circular economy in the agro-industrial sector, and new product design.

 | *Biofuels, Bioprod. Bioref*. (2024); DOI: 10.1002/bbb.2600